Electronic Supplementary Material (ESI) for Environmental Science: Atmospheres.

Cite this: DOI: 00.0000/xxxxxxxxxx

Supplementary Information: Comparison of Secondary Organic Aerosol Generated From the Oxidation of Laboratory Precursors by Hydroxyl Radicals, Chlorine Atoms, and Bromine Atoms in an Oxidation Flow Reactor

Andrew T. Lambe,*[a] Anita M. Avery[a], Nirvan Bhattacharyya[b], Dongyu S. Wang[b‡], Mrinali Modi[b], Catherine G. Masoud[b], Lea Hildebrandt Ruiz[b], and William H. Brune[c]

Received Date
Accepted Date

DOI: 00.0000/xxxxxxxxxx

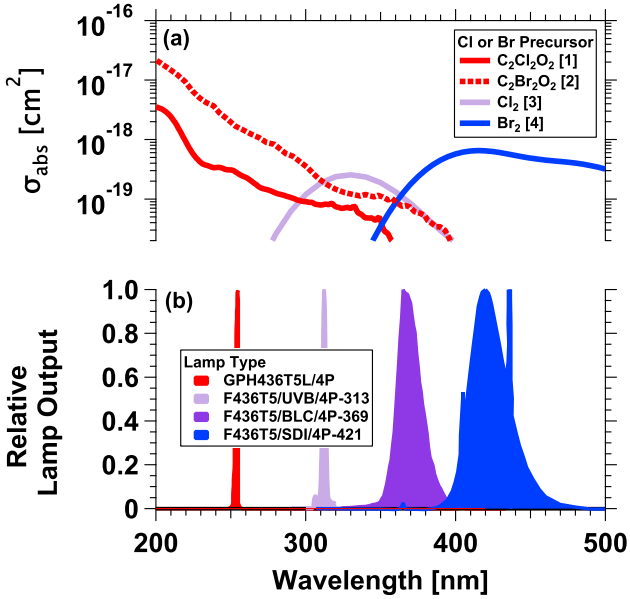

Fig. S1 (a) Absorption cross sections of Cl and Br precursors used in this study, with references as noted: [1] $C_2Cl_2O_2$ [1], [2] $C_2Br_2O_2$ [2,3], [3] Cl_2 [4], [4] Br_2 [5]. **(b)** Normalized emission spectra for low-pressure GPH436T5L/4P, F436T5/UVB/4P-313, F436T5/BLC/4P-369, and F436T5/SDI/4P-421 mercury lamps used in this study. Spectra are provided by the manufacturer (GPH436T5L/4P: Light Sources Inc.; all others: LCD Lighting, Inc.

[a] *Aerodyne Research Inc., Billerica, Massachusetts, USA; E-mail: lambe@aerodyne.com*
[b] *University of Texas at Austin, Austin, Texas, USA*
[c] *Pennsylvania State University, University Park, PA, USA*

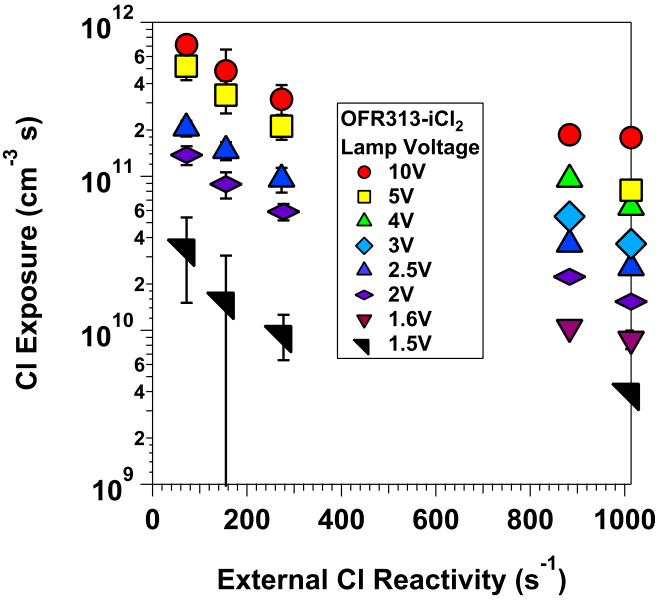

Fig. S2 Cl exposure calibration data obtained as a function of lamp voltage and external Cl reactivity for the OFR313-iCl$_2$ method. These data were obtained at τ_{OFR} = 130 s with 12 ppm Cl$_2$ injected into the OFR. Error bars represent $\pm 1\sigma$ in replicate measurements.

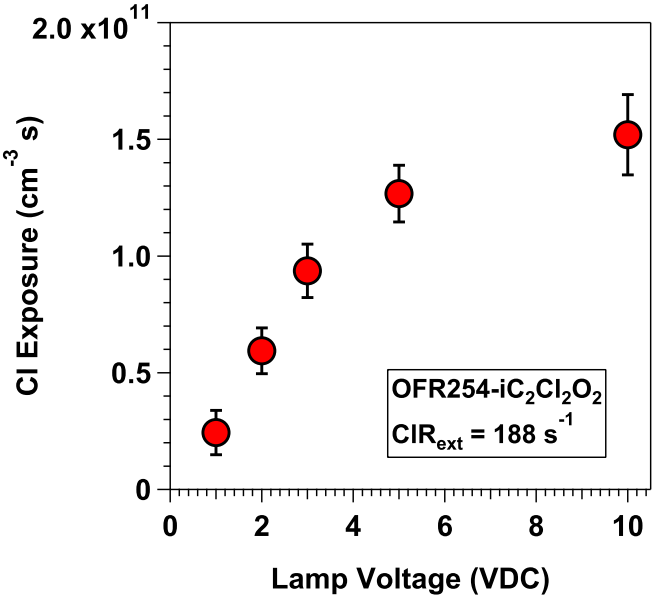

Fig. S3 Cl exposure calibration data obtained as a function of lamp voltage for the OFR254-iC$_2$Cl$_2$O$_2$ method. These data were obtained at τ_{OFR} = 90 s with 4.2 ppm C$_2$Cl$_2$O$_2$ and 636 ppb O$_3$ injected into the OFR. Error bars represent $\pm 1\sigma$ in replicate measurements.

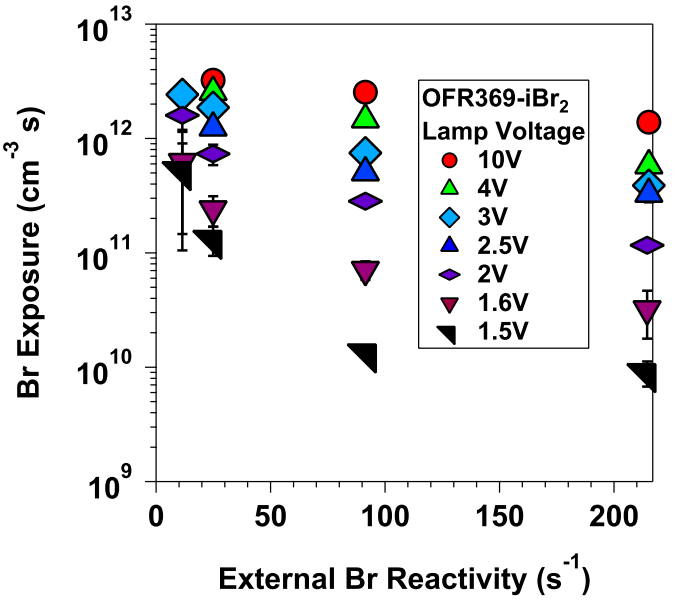

Fig. S4 Br exposure calibration data obtained as a function of lamp voltage and external Br reactivity for the OFR369-iBr$_2$ method. These data were obtained at τ_{OFR} = 130 s with 1.9 ppm Br$_2$ injected into the OFR. Error bars represent $\pm 1\sigma$ in replicate measurements.

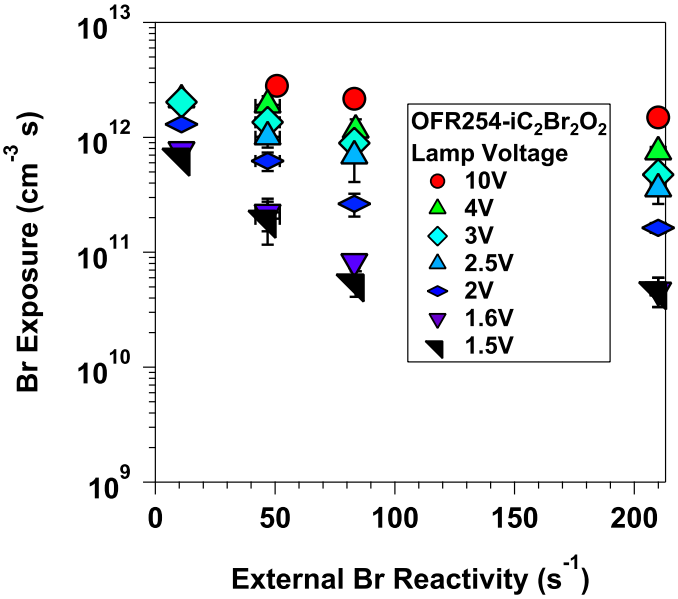

Fig. S5 Br exposure calibration data obtained as a function of lamp voltage and external Br reactivity for the OFR254-iC$_2$Br$_2$O$_2$ method. These data were obtained at τ_{OFR} = 130 s with 1.8 ppm C$_2$Br$_2$O$_2$ injected into the OFR. Error bars represent $\pm 1\sigma$ in replicate measurements.

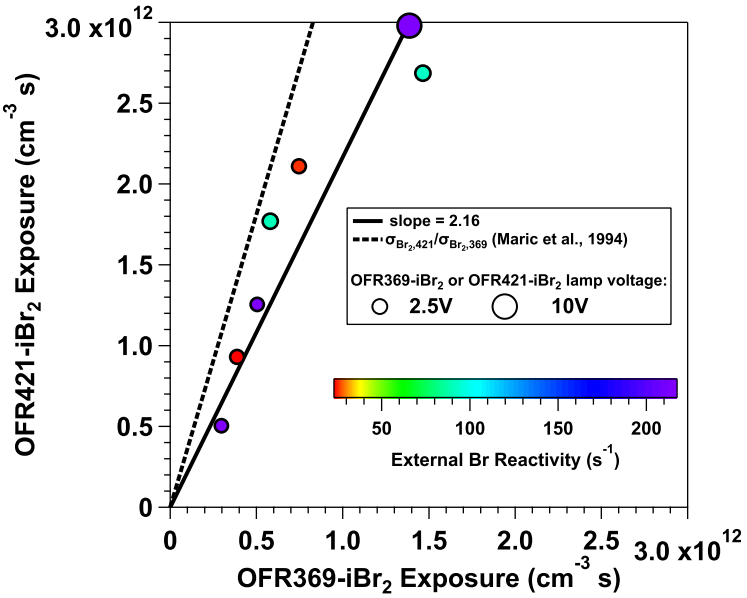

Fig. S6 Relationship between Br exposure obtained using OFR421-iBr_2 and OFR369-iBr_2 methods at equivalent lamp voltages and external Br reactivity values. Symbols are sized by lamp voltage and colored by external Br reactivity. The solid linear regression line has a slope of 2.16. The dashed line represents a line with a slope of Br_2 absorption cross sections at 369 and 421 nm from Maric *et al.* [5].

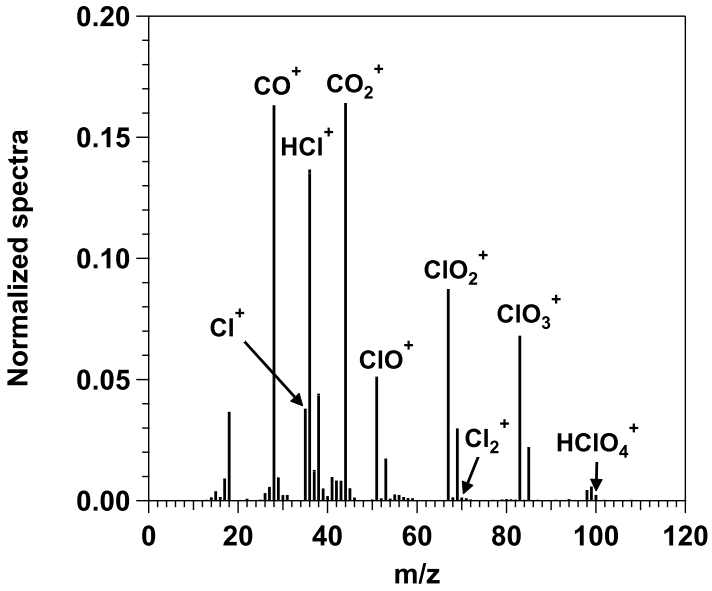

Fig. S7 L-ToF-AMS spectrum obtained during OFR conditioning with humidified air, O_3, and OH (generated using OFR185) immediately following Cl-OFR experiments conducted using OFR254-i$C_2Cl_2O_2$. Similar spectra were obtained after OFR185 conditioning following OFR313/369-iCl_2 studies.

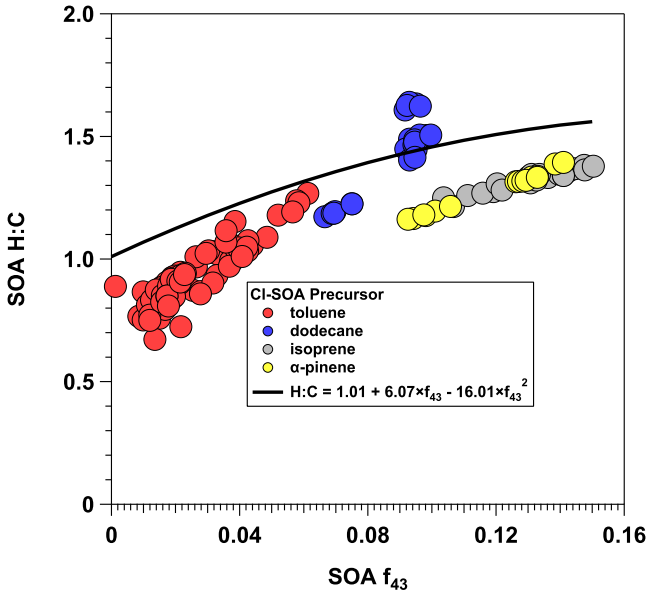

Fig. S8 Cl-SOA hydrogen-to-carbon (H/C) ratio as a function of the fraction of Cl-SOA signal measured at m/z = 43 (f_{43}). Here, H/C and f_{43} were obtained from L-ToF-AMS spectra. Solid black line is a quadratic regression line from Ng *et al.* [6].

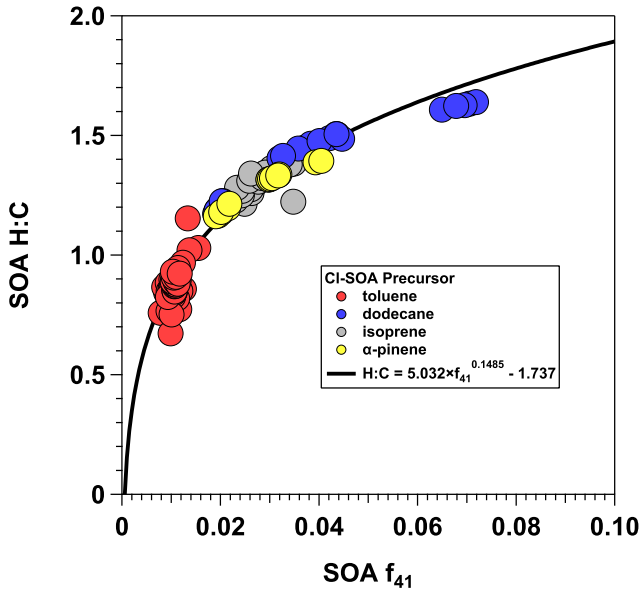

Fig. S9 Cl-SOA hydrogen-to-carbon (H/C) ratio as a function of the fraction of Cl-SOA signal measured at m/z = 41 (f_{41}). H/C and f_{41} were obtained from L-ToF-AMS spectra. Solid black line is a power law regression line fit to the data.

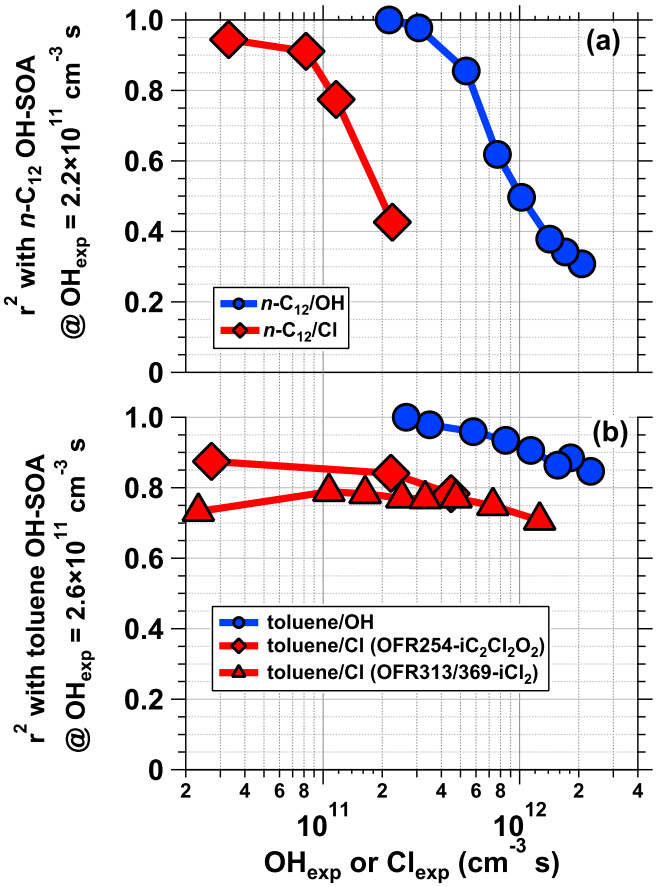

Fig. S10 Square of the Pearson correlation coefficient (r^2) between L-ToF-AMS spectra of **(a)** n-C_{12} OH-SOA generated at OH_{exp} = 2.2×10^{11} cm^{-3} s) and n-C_{12} OH-/Cl-SOA obtained as a function of OH_{exp} or Cl_{exp} **(b)** toluene OH-SOA generated at OH_{exp} = 2.6×10^{11} cm^{-3} s with toluene OH-/Cl-SOA spectra obtained as a function of OH_{exp} or Cl_{exp}.

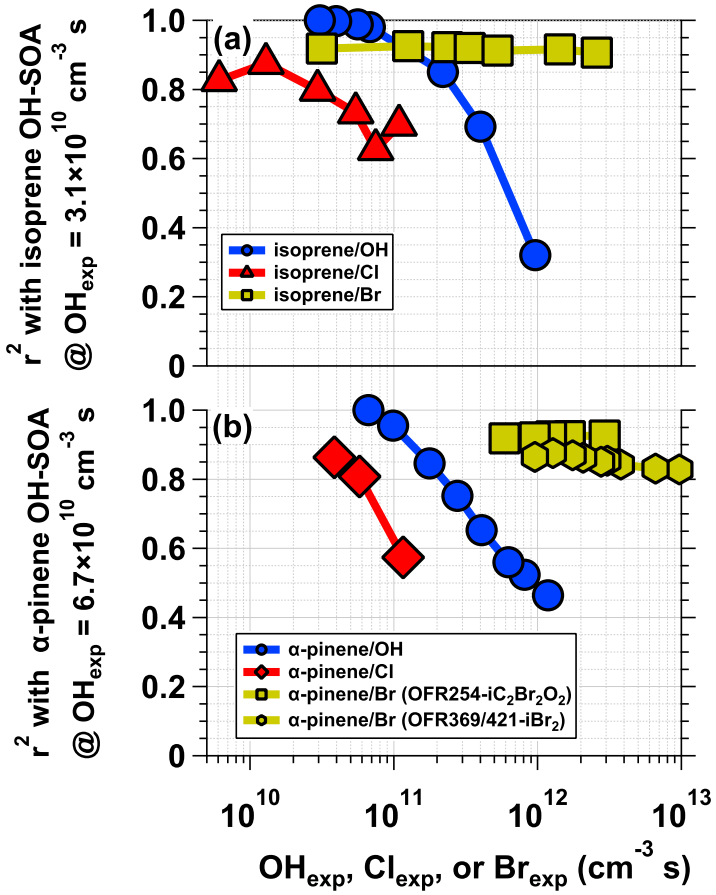

Fig. S11 Square of the Pearson correlation coefficient (r^2) between L-ToF-AMS spectra of **(a)** isoprene OH-SOA generated at OH_{exp} = 3.1×10^{10} cm^{-3} s) and isoprene OH-/Cl-/Br-SOA obtained as a function of OH_{exp}, Cl_{exp} or Br_{exp} **(b)** α-pinene OH-SOA generated at OH_{exp} = 6.7×10^{10} cm^{-3} s with α-pinene OH-/Cl-/Br-SOA spectra obtained as a function of OH_{exp}, Cl_{exp}, or Br_{exp}.

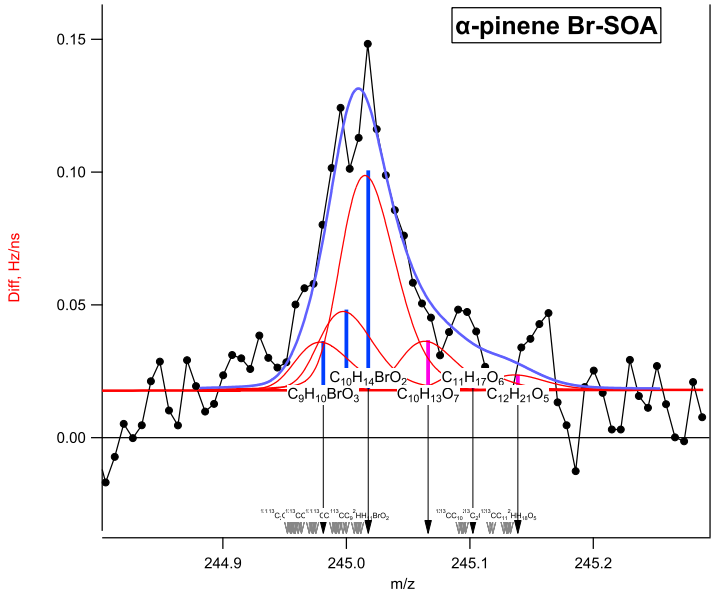

Fig. S12 High-resolution L-ToF-AMS spectrum of α-pinene Br-SOA at m/z = 245. Multiple ions were assigned to the peak at m/z=245, with the largest contribution coming from $C_{10}H_{14}BrO_2^+$, followed by $C_9H_{10}BrO_3^+$ and $C_{10}H_{12}{}^{81}BrO_2^+$.

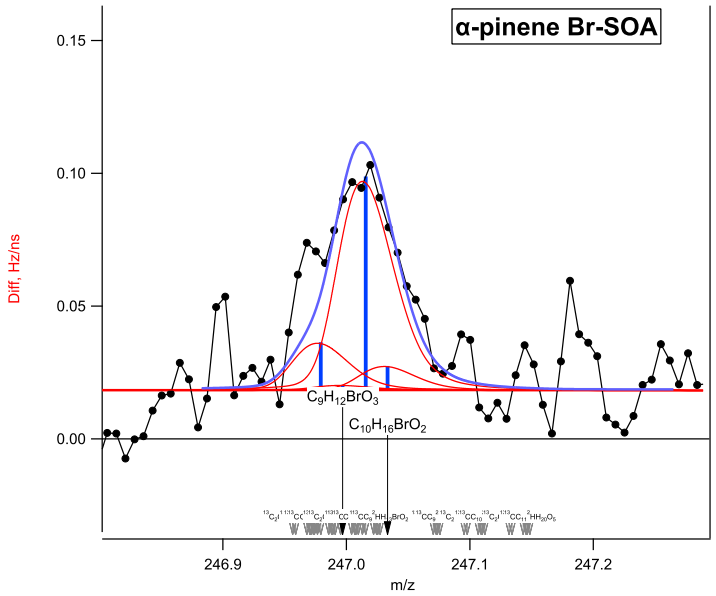

Fig. S13 High-resolution L-ToF-AMS spectrum of α-pinene Br-SOA at m/z = 247. Multiple ions were assigned to the peak at m/z=247, with the largest contribution coming from $C_{10}H_{14}$ $^{81}BrO_2^+$, followed by $C_9H_{12}BrO_3^+$ and $C_{10}H_{16}BrO_2^+$.

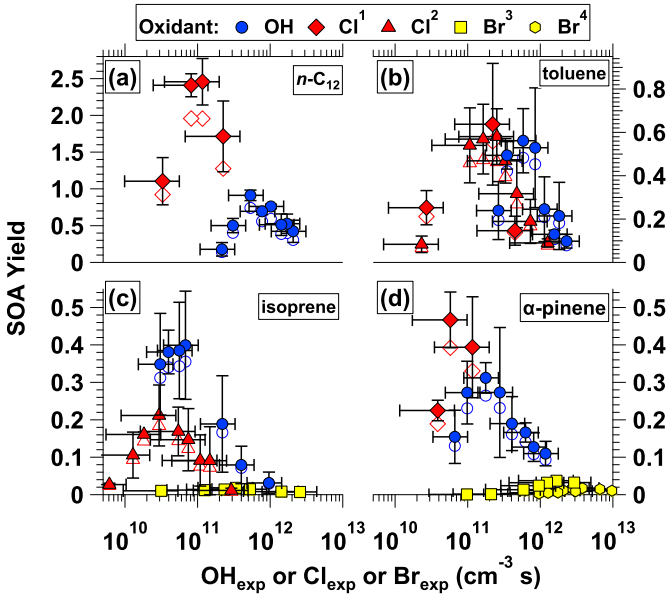

Fig. S14 Mass yields of SOA generated from **(a)** OH and Cl oxidation of *n*-C_{12}, **(b)** OH and Cl oxidation of toluene, **c** OH, Cl, and Br oxidation of isoprene, and **(d)** OH, Cl, and Br oxidation of α-pinene as a function of OH_{exp}, Cl_{exp}, or Br_{exp}. Closed symbols represent SOA yield values with particle wall loss correction factors applied; open symbols represent the same data without particle wall loss correction factors. Different y-axis scales are used in each subpanel. Error bars indicate $\pm 1\sigma$ uncertainty in binned SOA yield values, $\pm$50% uncertainty in OH exposure values, and $\pm$70% uncertainty in Cl and Br exposure values. Additional figure notes: [1]Cl generated using OFR254/313-i$C_2Cl_2O_2$; [2]Cl generated using OFR313/369-iCl_2; [3]Br generated using OFR254-i$C_2Br_2O_2$; [4]Br generated using OFR369/421-iBr_2.

Table S1 KinSim mechanism used to model Cl and Br formation and destruction in the OFR.

Reactant 1	Reactant 2	Product 1	Product 2	Product 3	A_∞	E_∞	n_∞	A_0	E_0	n_0	References
Cl_2	HV254	2 Cl			7.26×10^{-22}	0	0	0	0	0	4
Cl_2	HV313	2 Cl			2.032×10^{-19}	0	0	0	0	0	4
Cl_2	HV369	2 Cl			8.828×10^{-20}	0	0	0	0	0	4
Cl_2	$O(^1D)$	Cl_2	$O(^3P)$		2.19×10^{-10}	0	0	0	0	0	7
Cl_2	$O(^1D)$	ClO	Cl		1.99×10^{-10}	0	0	0	0	0	8
Cl_2	$O(^3P)$	ClO	Cl		4.17×10^{-12}	1370	0	0	0	0	9
Cl_2	OH	HOCl	Cl		3.6×10^{-12}	1200	0	0	0	0	9
Cl_2	Cl	Cl_3			1.51×10^{-16}	0	0	0	0	0	10
Cl_2	Br	BrCl	Cl		1.1×10^{-15}	0	0	0	0	0	11
Cl_2	ClCO	$COCl_2$	Cl		4.18×10^{-12}	1490.14	0	0	0	0	12
$C_2Cl_2O_2$	HV254	2 Cl	2 CO		2.76×10^{-19}	0	0	0	0	0	1
$C_2Cl_2O_2$	HV313	2 Cl	2 CO		8.19×10^{-20}	0	0	0	0	0	1
$C_2Cl_2O_2$	Cl	Cl_2	CO	COCl	4×10^{-14}	0	0	0	0	0	13
Br_2	HV369	2 Br			1.78×10^{-19}	0	0	0	0	0	5
Br_2	HV421	2 Br			6.45×10^{-19}	0	0	0	0	0	5
Br_2	$O(^3P)$	BrO	Br		5.11×10^{-13}	-989	0	0	0	0	14
Br_2	OH	Br	HOBr		2×10^{-11}	240.558	0	0	0	0	9
Br_2	Cl	Br	BrCl		2.3×10^{-10}	134.713	0	0	0	0	15
$C_2Br_2O_2$	HV254	2 Br	2 CO		1.68×10^{-18}	0	0	0	0	0	3
$C_2Br_2O_2$	Br	Br_2	CO	COBr	4×10^{-14}	0	0	0	0	0	16
O_3	HV254	O_2	$O(^1D)$		1.03×10^{-17}	0	0	0	0	0	17
O_3	HV313	O_2	$O(^1D)$		6.84×10^{-20}	0	0	0	0	0	17
O_3	HV369	O_2	$O(^1D)$		3.59×10^{-23}	0	0	0	0	0	17
O_3	HV421	O_2	$O(^1D)$		6.47×10^{-23}	0	0	0	0	0	17
O_3	Cl	ClO	O_2		2.3×10^{-11}	200	0	0	0	0	9
O_3	ClO	O_2	OClO		1×10^{-18}	0	0	0	0	0	9
O_3	ClO	O_2	ClOO		1.5×10^{-17}	0	0	0	0	0	9
O_3	OClO	O_2	ClO_3		2.1×10^{-12}	4700	0	0	0	0	9
O_3	Cl_2O_2	O_2	ClOO	ClO	1×10^{-19}	0	0	0	0	0	9
O_3	Br	O_2	BrO		1.7E-11	799.856	0	0	0	0	9
O_3	BrO	2 O_2	Br		2E-17	0	0	0	0	0	18
O_3	BrO_2				5E-16	0	0	0	0	0	19
Cl	OH	HCl	$O(^3P)$		9.8×10^{-12}	2860.24	0	0	0	0	20
Cl	HO_2	HCl	O_2		1.4×10^{-11}	-270	0	0	0	0	9
Cl	HO_2	OH	ClO		6.3×10^{-11}	570.123	0	0	0	0	9
Cl	Cl	Cl_2			6.15E-34	-905.701	0	0	0	0	20
Cl	O_2	ClOO			0	0	0	1.4×10^{-33}	0	3.9	9
Cl	H_2	HCl	H		3.9×10^{-11}	2310.56	0	0	0	0	9
Cl	H_2O_2	HCl	HO_2		1.1×10^{-11}	980	0	0	0	0	9
Cl	CO	ClCO			3.4×10^{-14}	0	0	0	0	0	21
ClCO		Cl	CO		4.1×10^{-10}	2960.07	0	0	0	0	9
Cl	ClCO	Cl_2	CO		2.16×10^{-9}	1670.68	0	0	0	0	20
ClO	HV254	Cl	$O(^3P)$		4.25×10^{-18}	0	0	0	0	0	22
ClO	HV313	Cl	$O(^3P)$		3.25×10^{-19}	0	0	0	0	0	22
ClO	$O(^3P)$	Cl	O_2		2.5×10^{-11}	-109.454	0	0	0	0	9
ClO	OH	HCl	O_2		1.2×10^{-12}	0	0	0	0	0	9
ClO	OH	HO_2	Cl		1.9×10^{-11}	0	0	0	0	0	9
ClO	HO_2	O_2	HOCl		4.8×10^{-13}	700.024	0	0	0	0	23
ClO	HO_2	HCl	O_3		2.01×10^{-14}	0	0	0	0	0	24
ClO	Cl	Cl_2	$O(^3P)$		1.74×10^{-12}	4589.85	0	0	0	0	20
ClO	ClO	OClO	Cl		3.5×10^{-13}	1370	0	0	0	0	9
ClO	ClO	Cl_2O_2			1×10^{-11}	0	0	2.05×10^{-32}	0	4	9

Table S1 KinSim mechanism used to model Cl and Br formation and destruction in the OFR (continued).

ClO	ClO	ClOO	Cl		8.06×10^{-15}	0	0	0	0	0	9
ClO	ClO	O_2	2 Cl		3×10^{-11}	2450	0	0	0	0	25
ClO	ClO	O_2	Cl_2		1×10^{-12}	1590	0	0	0	0	9
ClO	BrO	OClO	Br		1.6×10^{-12}	-430.599	0	0	0	0	9
ClO	BrO	ClOO	Br		2.9×10^{-12}	-220.111	0	0	0	0	9
ClO	BrO	BrCl	O_2		5.8×10^{-13}	-169.593	0	0	0	0	9
OClO	HV254	ClO	$O(^3P)$		3.49×10^{-19}	0	0	0	0	0	22
OClO	HV313	ClO	$O(^3P)$		1.74×10^{-18}	0	0	0	0	0	22
OClO	HV369	ClO	$O(^3P)$		9.03×10^{-18}	0	0	0	0	0	22
OClO	$O(^3P)$	ClO	O_2		2.4×10^{-12}	960	0	0	0	0	9
OClO	$O(^3P)$	ClO_3			3.11×10^{-11}	0	1	1.91E-31	0	0	9
OClO	OH	O_2	HOCl		1.4×10^{-12}	-600	0	0	0	0	9
OClO	Cl	2 ClO			3.2×10^{-11}	-169.593	0	0	0	0	9
OClO	ClO	Cl_2O_3			2.4×10^{-11}	0	0	6.2×10^{-32}	0	4.7	9
OClO	Br	ClO	BrO		2.7×10^{-11}	1300.22	0	0	0	0	9
ClOO	HV254	ClO	$O(^3P)$		1.24×10^{-17}	0	0	0	0	0	26
ClOO		Cl	O_2		0	0	0	2.8×10^{-10}	1820	0	9
ClOO	H	ClO	OH		5.65×10^{-11}	0	0	0	0	0	20
ClOO	$O(^3P)$	ClO	O_2		4.98×10^{-11}	0	0	0	0	0	27
ClOO	Cl	Cl_2	O_2		2.3×10^{-10}	0	0	0	0	0	23
ClOO	Cl	2 ClO			1.2×10^{-11}	0	0	0	0	0	23
ClOO	Br	O_2	BrCl		5.15×10^{-14}	0	0	0	0	0	28
Cl_2O	HV254	ClO	Cl		1.84×10^{-18}	0	0	0	0	0	29,30
Cl_2O	HV313	Cl_2	Cl		3.94×10^{-19}	0	0	0	0	0	29,30
Cl_2O	HV369	Cl_2	Cl		5.43×10^{-21}	0	0	0	0	0	29,30
Cl_2O	H	ClO	HCl		4.1×10^{-11}	0	0	0	0	0	31
Cl_2O	$O(^3P)$	2 ClO			2.7×10^{-11}	530	0	0	0	0	9
Cl_2O	OH	HOCl	ClO		5.1×10^{-12}	-100	0	0	0	0	32
Cl_2O	Cl	Cl_2	ClO		6.20×10^{-11}	129.901	0	0	0	0	9
Cl_2O	ClO	Cl_2	ClOO		4.32×10^{-16}	0	0	0	0	0	27
Cl_2O	ClO	Cl_2	Cl	O_2	1.08×10^{-15}	0	0	0	0	0	27
Cl_2O	Br	ClO	BrCl		2.1×10^{-11}	470.291	0	0	0	0	9
Cl_2O_2	HV254	ClOO	Cl		6.01×10^{-18}	0	0	0	0	0	30,33
Cl_2O_2	HV313	ClOO	Cl		3.81×10^{-19}	0	0	0	0	0	30,33
Cl_2O_2	HV369	ClOO	Cl		4.76×10^{-20}	0	0	0	0	0	30,33
Cl_2O_2		2 ClO			3.7×10^{-7}	7690.64	0	0	0	0	9
Cl_2O_2	OH	HOCl	ClOO		6×10^{-13}	-670	0	0	0	0	32
Cl_2O_2	Cl	Cl_2	ClOO		7.6×10^{-11}	-65	0	0	0	0	9
Cl_2O_2	Br	ClOO	BrCl		5.9×10^{-12}	169.593	0	0	0	0	9
Cl_2O_3	HV254				1.443×10^{-17}	0	0	0	0	0	22
Cl_2O_3	HV313				1.86×10^{-18}	0	0	0	0	0	22
Cl_2O_3		ClO	OClO		1.4×10^{-10}	3810.44	0	0	0	0	9
BrO	HV369	Br	$O(^3P)$		1.01×10^{-18}	0	0	0	0	0	34
BrO	$O(^3P)$	BrO_2			5×10^{-11}	0	0	0	0	0	34
BrO	$O(^3P)$	Br	O_2		1.9×10^{-11}	-230	0	0	0	0	9
BrO	OH	O_2	HBr		1×10^{-12}	0	0	0	0	0	35
BrO	OH				1.8×10^{-11}	-250.18	0	0	0	0	9
BrO	HO_2	O_2	HOBr		6.19×10^{-12}	500.361	0	0	0	0	36
BrO	BrO	Br	BrO_2		5.25×10^{-11}	449.844	0	0	0	0	37
BrO	BrO	O_2	2 Br		2.7×10^{-12}	0	0	0	0	0	9
BrO	BrO	Br_2	O_2		2.5×10^{-14}	0	0	0	0	0	9
BrO_2	HV421	BrO	$O(^3P)$		5.70×10^{-18}	0	0	0	0	0	22
BrO_2	$O(^3P)$	BrO	O_2		4.25×10^{-12}	0	0	0	0	0	34

Table S1 KinSim mechanism used to model Cl and Br formation and destruction in the OFR (continued).

BrO_2	Br			5×10^{-11}	0	0	0	0	0	34
BrO_2	ClO			1.5×10^{-13}	0	0	0	0	0	38
BrO_2	OClO			6×10^{-14}	0	0	0	0	0	38
HCl	H	H_2	Cl	1.32×10^{-11}	1710.37	0	0	0	0	20
HCl	$O(^1D)$	Cl	OH	1×10^{-10}	0	0	0	0	0	39
HCl	$O(^1D)$	ClO	H	3.6×10^{-11}	0	0	0	0	0	39
HCl	$O(^3P)$	Cl	OH	1×10^{-11}	3300	0	0	0	0	23
HCl	OH	Cl	H_2O	1.72×10^{-12}	229.733	0	0	0	0	9
HOCl	HV254	OH	Cl	1.46×10^{-19}	0	0	0	0	0	40
HOCl	HV313	OH	Cl	5.84×10^{-20}	0	0	0	0	0	40
HOCl	HV369	OH	Cl	9.19×10^{-21}	0	0	0	0	0	40
HOCl	H	HCl	OH	6.71×10^{-13}	0	0	0	0	0	41
HOCl	$O(^3P)$	ClO	OH	1.7×10^{-13}	0	0	0	0	0	9
HOCl	OH	ClO	H_2O	3.01×10^{-12}	500	0	0	0	0	23
HOCl	Cl	ClO	HCl	3.4×10^{-12}	130	0	0	0	0	23
HOCl	Cl	OH	Cl_2	3.4×10^{-13}	0	0	0	0	0	41
HBr	H	Br	H_2	8.32×10^{-12}	81.7898	1.05	0	0	0	42
HBr	$O(^1D)$			1.5×10^{-10}	0	0	0	0	0	23
HBr	$O(^3P)$	Br	OH	5.8×10^{-12}	1500	0	0	0	0	23
HBr	OH	Br	H_2O	6.7×10^{-12}	-155.16	0	0	0	0	9
HBr	Cl	Br	HCl	7.8×10^{-12}	0	0	0	0	0	20
HBr	ClO	Br	HOCl	5.60×10^{-15}	0	0	0	0	0	43
HBr	BrO	Br	HOBr	6.19×10^{-15}	0	0	0	0	0	43
HOBr	HV254	OH	Br	6.19×10^{-20}	0	0	0	0	0	22
HOBr	HV369	OH	Br	9.32×10^{-20}	0	0	0	0	0	22
HOBr	HV421	OH	Br	9.67×10^{-21}	0	0	0	0	0	22
HOBr	$O(^3P)$	BrO	OH	1.2×10^{-10}	430.6	0	0	0	0	9
HOBr	OH			5×10^{-13}	0	0	0	0	0	44
HOBr	Cl	BrCl	OH	8×10^{-11}	0	0	0	0	0	44
BrCl	HV254	Br	Cl	3.24×10^{-20}	0	0	0	0	0	5
BrCl	HV313	Br	Cl	2.51×10^{-20}	0	0	0	0	0	5
BrCl	HV369	Br	Cl	3.96×10^{-19}	0	0	0	0	0	5
BrCl	HV421	Br	Cl	1.78×10^{-19}	0	0	0	0	0	5
BrCl	$O(^3P)$	BrO	Cl	2.09×10^{-11}	0	0	0	0	0	45
BrCl	OH			1.5×10^{-12}	0	0	0	0	0	44
BrCl	Cl	Cl_2	Br	1.45×10^{-11}	0	0	0	0	0	46
BrCl	Br	Br_2	Cl	3.32×10^{-15}	0	0	0	0	0	20

References

1 B. Ghosh, D. K. Papanastasiou and J. B. Burkholder, *The Journal of Chemical Physics*, 2012, **137**, 164315.

2 J. E. Tuttle and G. K. Rollefson, *J. Am. Chem. Soc.*, 1941, **63**, 1525–1530.

3 H. Shimada, R. Shimada and Y. Kanda, *Bulletin of the Chemical Society of Japan*, 1968, **41**, 1289–1295.

4 D. Maric, J. Burrows, R. Meller and G. Moortgat, *Journal of Photochemistry and Photobiology A: Chemistry*, 1993, **70**, 205 – 214.

5 D. Maric, J. Burrows and G. Moortgat, *Journal of Photochemistry and Photobiology A: Chemistry*, 1994, **83**, 179 – 192.

6 N. L. Ng, M. R. Canagaratna, J. L. Jimenez, P. S. Chhabra, J. H. Seinfeld and D. R. Worsnop, *Atmospheric Chemistry and Physics*, 2011, **11**, 6465–6474.

7 I. S. Fletcher and D. Husain, *Berichte der Bunsengesellschaft für physikalische Chemie*, 1976, **80**, 982–985.

8 K. Freudenstein and D. Biedenkapp, *Colloid and Polymer Science*, 1977, **255**, 928–928.

9 R. Atkinson, D. L. Baulch, R. A. Cox, J. N. Crowley, R. F. Hampson, R. G. Hynes, M. E. Jenkin, M. J. Rossi and J. Troe, *Atmospheric Chemistry and Physics*, 2007, **7**, 981–1191.

10 E. Hutton and M. Wright, *Trans. Faraday Soc.*, 1965, **61**, 78–89.

11 D. A. Dolson and S. R. Leone, *The Journal of Physical Chemistry*, 1987, **91**, 3543–3550.

12 W. G. Burns and F. S. Dainton, *Trans. Faraday Soc.*, 1952, **48**, 39–52.

13 A. V. Baklanov and L. N. Krasnoperov, *J. Phys. Chem. A*, 2001, **105**, 97–103.

14 M. H. Harwood, D. M. Rowley, R. A. Cox and R. L. Jones, *J. Phys. Chem. A*, 1998, **102**, 1790–1802.

15 Y. Bedjanian, G. Laverdet and G. Le Bras, *J. Phys. Chem. A*, 1998, **102**, 953–959.

16 C.-C. Wu, H.-C. Lin, Y.-B. Chang, P.-Y. Tsai, Y.-Y. Yeh, H. Fan, K.-C. Lin and J. S. Francisco, *The Journal of Chemical Physics*, 2011, **135**, 234308.

17 J. Burrows, A. Richter, A. Dehn, B. Deters, S. Himmelmann, S. Voigt and J. Orphal, *Journal of Quantitative Spectroscopy and Radiative Transfer*, 1999, **61**, 509–517.

18 R. Atkinson, D. Baulch, R. Cox, J. Crowley, J. Hampson, R.F, J. Kerr, M. Rossi and J. Troe, *IUPAC Subcommittee on Gas Kinetic Data Evaluation for Atmospheric Chemistry - Web Version*, 2001.

19 Z. Li, *J. Phys. Chem. A*, 1999, **103**, 1206–1213.

20 D. L. Baulch, J. Duxbury, S. J. Grant and D. C. Montague, *J. Phys. Chem. Ref. Data*, 1981, **10**, year.

21 A. D. Hewitt, K. M. Brahan, G. D. Boone and S. A. Hewitt, *International Journal of Chemical Kinetics*, 1996, **28**, 763–771.

22 S. Sander, R. Friedl, D. Golden, M. Kurylo, G. Moortgat, H. Keller-Rudek, P. Wine, A. R. Ravishankara, C. Kolb, M. Molina, B. Finlayson-Pitts, R. Huie and V. Orkin, *JPL Publication*, 2006, 1–523.

23 W. B. DeMore, S. P. Sander, D. M. Golden, R. F. Hampson, M. J. Kurylo, C. J. Howard, A. R. Ravishankara, C. E. Kolb and M. J. Molina, *JPL Publication 97-4*, 1997.

24 R. Atkinson, D. L. Baulch, R. A. Cox, R. F. Hampson, J. A. Kerr (Chairman) and J. Troe, *Journal of Physical and Chemical Reference Data*, 1989, **18**, 881–1097.

25 A. Horowitz, D. Bauer, J. N. Crowley and G. K. Moortgat, *Geophysical Research Letters*, 1993, **20**, 1423–1426.

26 H. S. Johnston, E. D. Morris and J. Van den Bogaerde, *J. Am. Chem. Soc.*, 1969, **91**, 7712–7727.

27 N. Basco, S. K. Dogra and R. G. W. Norrish, *Proceedings of the Royal Society of London. A. Mathematical and Physical Sciences*, 1971, **323**, 401–415.

28 M. A. A. Clyne, J. A. Coxon and J. W. Linnett, *Proceedings of the Royal Society of London. Series A. Mathematical and Physical Sciences*, 1967, **298**, 424–452.

29 C. M. Nelson, T. A. Moore, M. Okumura and T. K. Minton, *The Journal of Chemical Physics*, 1994, **100**, 8055–8064.

30 D. K. Papanastasiou, K. J. Feierabend and J. B. Burkholder, *The Journal of Chemical Physics*, 2011, **134**, 204310.

31 S. J. Wategaonkar and D. W. Setser, *The Journal of Chemical Physics*, 1989, **90**, 251–264.

32 J. C. Hansen, R. R. Friedl and S. P. Sander, *J. Phys. Chem. A*, 2008, **112**, 9229–9237.

33 T. A. Moore, M. Okumura, J. W. Seale and T. K. Minton, *J. Phys. Chem. A*, 1999, **103**, 1691–1695.

34 N. Butkovskaya, I. Morozov, V. Tal'rose and E. Vasiliev, *Chemical Physics*, 1983, **79**, 21–30.

35 Y. Bedjanian, V. Riffault, G. Le Bras and G. Poulet, *J. Phys. Chem. A*, 2001, **105**, 6154–6166.

36 W. DeMore, S. Sander, D. Golden, R. Hampson, M. Kurylo, C. Howard, A. Ravishankara, C. Kolb and M. Molina, *JPL Publication 94-26*, 1994.

37 M. A. A. Clyne and H. W. Cruse, *Trans. Faraday Soc.*, 1970, **66**, 2214–2226.

38 Z. Li, G. R. Jeong and E. C. Person, *International Journal of Chemical Kinetics*, 2002, **34**, 430–437.

39 A. Chichinin, *Chemical Physics Letters - CHEM PHYS LETT*, 2000, **316**, 425–432.

40 R. J. Barnes, A. Sinha and H. A. Michelsen, *J. Phys. Chem. A*, 1998, **102**, 8855–8859.

41 R. Vogt and R. N. Schindler, *Berichte der Bunsengesellschaft für physikalische Chemie*, 1993, **97**, 819–829.
42 M. Seakins, P.W.; Pilling, *J. Phys. Chem.*, 1991, 9878–9881.
43 A. A. Turnipseed, J. W. Birks and J. G. Calvert, *J. Phys. Chem.*, 1991, **95**, 4356–4364.
44 A. Kukui, U. Kirchner, T. Benter and R. N. Schindler, *ChemInform*, 1996, **27**, year.
45 M. A. A. Clyne, P. B. Monkhouse and L. W. Townsend, *International Journal of Chemical Kinetics*, 1976, **8**, 425–449.
46 M. A. A. Clyne and H. W. Cruse, *J. Chem. Soc., Faraday Trans. 2*, 1972, **68**, 1377–1387.